thermal sintering, besides adding new redox properties to it.

The IR studies of the surface hydroxy groups as well as of the surface complexes obtained by carbon monoxide and pyridine adsorption support and complete the criteria for the identification of surface sites on metal oxide surfaces, previously discussed by us,[17] arising from slight modifications of those of Knozinger and Ratnasami[39] for surface OH's and of Morterra et al. for Lewis acid sites.[48] In particular, it is confirmed that the presence of cationic vacancy clusters with respect to the spinel stoichiometry on the defective spinel aluminas and on bivalent-deficient aluminate spinels produces typical surface sites, absent on stoichiometric spinels.

IR data indicate that the surface composition of the mixed oxides $Ni_xAl_{2-2x}O_{3-2x}$ substantially reflects that of the bulk. In fact evidence of the presence at the surface of sites arising from all structures observed in the bulk has been provided. This is also the case of the Ni085 powder, found to be constituted by a monophasic rock salt type structure, whose unit cell is slightly contracted with respect to that of NiO as the result of the presence of relevant amounts of Al^{3+} in both tetrahedral and octahedral environments. The surface of this material is strongly modified with respect to that of pure NiO, showing complex νOH spectra and strong Lewis acid sites as the result of the presence of Al^{3+} ions in both tetrahedral and octahedral unsaturated coordination also at the surface. The higher thermal stability of pyridine adsorbed on it would also evidence a deep modification of its electronic properties with respect to NiO.

The present study also shows that $NiAl_2O_4$ prepared by sodium carbonate is contaminated by Na^+ ions at the surface, where tetrahedral Al^{3+} ions, responsible for strong Lewis acidity, are lacking or are poisoned. These sites are instead observed on samples prepared by ammonium carbonate coprecipitation.

Acknowledgment. The technical collaboration of R. Guidetti and C. Marcel is gratefully acknowledged. This work has been supported by MURST.

Registry No. $Ni_6Al_2(OH)_{16}(CO_3)\cdot 4H_2O$, 140468-28-6; Al_2O_3, 1344-28-1; $Ni_{0.33}Al_{1.34}O_{2.34}$, 140437-92-9; $Ni_{0.5}AlO_2$, 12004-35-2; $Ni_{0.85}Al_{0.3}O_{1.3}$, 140437-91-8; NiO, 1313-99-1; Na, 7440-23-5; CO, 630-08-0; boehmite, 1318-23-6; pyridine, 110-86-1; nitrogen, 7727-37-9; spinel, 12004-35-2.

Squaraine Chemistry. Design, Synthesis, and Xerographic Properties of a Highly Sensitive Unsymmetrical Fluorinated Squaraine

Kock-Yee Law

Xerox Webster Research Center, 800 Phillips Road, 0114-39D, Webster, New York 14580

Received October 29, 1991. Revised Manuscript Received February 17, 1992

A novel unsymmetrical fluorinated squaraine (UFSq), 3,4-dimethoxyphenyl-2′-fluoro-4′-(dimethylamino)phenylsquaraine, which was designed to improve the spectral sensitivity of squaraine in the visible region has been synthesized. The effects of synthesis and purification on the xerographic properties have been examined. Direct or indirect condensation of 1-(3′,4′-dimethoxyphenyl)-2-hydroxycyclobutene-3,4-dione with 3-fluoro-*N*,*N*-dimethylaniline affords UFSq in very similar chemical yields. The physical, morphological, and xerographic properties of UFSq samples from both routes are very similar also. Purification of UFSq by solvent extraction improves the purity of the as-synthesized UFSq samples. It was concluded, based on melting points and xerographic data, that CH_2Cl_2 extraction produces the "cleanest" sample for xerographic photoreceptor application. A bilayer device containing UFSq (CH_2Cl_2 purified) was shown to exhibit a low dark decay value (−15 V/s) and high panchromatic photosensitivity from the visible to the near-IR regions. The energies required to photodischarge half of the initial surface potential are 3.1 and 1.9 ergs/cm^2 at 600 and 790 nm, respectively. This sensitivity performance surpasses the sensitivity of all known squaraines and makes UFSq one of the most sensitive IR photoconducors known to date. Evidence is provided that the high sensitivity may be the result of the high purity and the high efficiency of hole injection of UFSq, from the charge generation layer to the charge-transporting layer, in the xerographic device. The electrical stability of UFSq is excellent. We have been able to show that the charging/photodischarging properties of an UFSq device remain unchanged after 50 000 cycles. This xerographic performance suggests that UFSq should be usable for diode laser (780 nm) and LED (660–680 nm) printers as well as copiers and multifunction printer-copiers.

Introduction

Bis(4-(dimethylamino)phenyl)squaraine (HSq) and many of its derivatives are organic photoconductors known to be usable in xerographic photoreceptors.[1,2] In solution, these compounds absorb at ~620–670 nm, depending on the substituent at the nitrogen and in the phenyl ring.[3] In the solid state, owing to the strong intermolecular donor–acceptor charge-transfer interactions, their absorptions

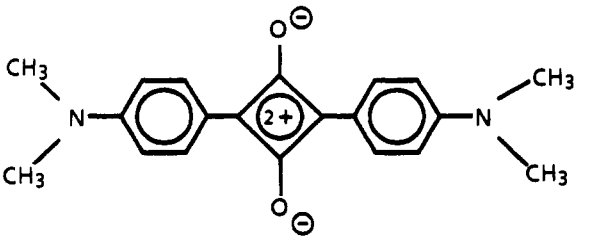

HSq

become very broad, typically exhibiting two bands, one in the visible region at 550–650 nm and the other in the

(1) Law, K. Y. *J. Imaging Sci.* **1987**, *31*, 83.
(2) Law, K. Y.; Bailey, F. C. *J. Imaging Sci.* **1987**, *31*, 172.
(3) Law, K. Y. *J. Phys. Chem.* **1987**, *91*, 5184.

0897-4756/92/2804-0605$03.00/0

near-IR region at 700–800 nm.[4] This optical characteristic makes squaraines particularly attractive as photogeneration pigments for IR photoreceptors in diode laser printers. One of the drawbacks in the optical absorption of squaraine is the low absorptivity at 400–500 nm. This low absorptivity has resulted in a lower spectral sensitivity in this region.[5] It implies that squaraine-based photoreceptors would not be suitable for high-quality copier applications, where a flat photoresponse in the visible region (400–650 nm) is essential.

HSq and its derivatives are traditionally synthesized by condensation of squaric acid with 2 equiv of *N,N*-dimethylaniline derivatives.[6] This procedure often produces squaraines that exhibit low charge-accepting properties and high dark conductivity in layered xerographic devices.[2] Two modified procedures, using the mono- and the dialkyl ester of squaric acid as precursors, have recently been developed to circumvent the performance problem.[2,7,8] The common starting material for these procedures is squaric acid which, by itself, has to be prepared by a multistep low yield reaction.[9] A procedure to simplify the squaraine synthesis is highly desirable. The objectives of our work are 2-fold: We plan to develop new synthetic procedures for squaraines so that they can be prepared without using squaric acid. We also plan to synthesize squaraines with high and flat photoresponse from 400 to 800 nm, so that they can be used in copiers, printers, and multifunction printer-copiers.

To meet these objectives, we have designed and synthesized a new class of unsymmetrical squaraines, namely, 4-methoxyphenyl-4′-(dimethylamino)phenylsquaraine and its derivatives, by a (2 + 2) cycloaddition/condensation reaction sequence.[10] Details on the rationale of the design

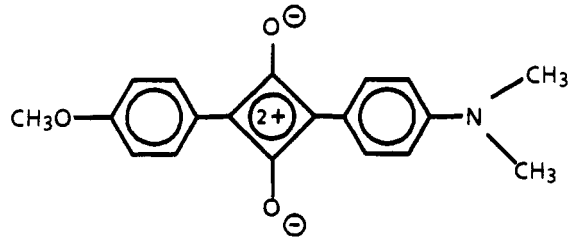

4-methoxyphenyl-4′-(dimethylamino)phenylsquaraine

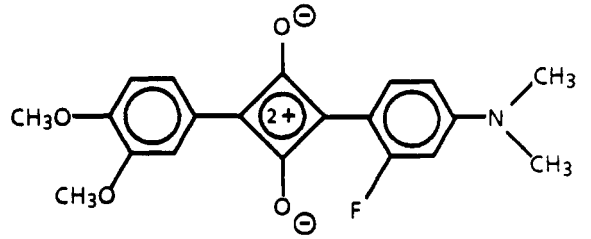

UFSq

and the synthetic strategy are described in a separate report.[11] Among the unsymmetrical squaraines reported, UFSq was identified as the most sensitive compound. Here the effects of synthesis and purification on the solid-state properties, morphological properties, and xerographic properties of UFSq are reported. Our data show that UFSq exhibits a flat and high photoresponse in the visible spectral region in xerographic devices. The peak sensitivity is at 790 nm. The goals of developing a new procedure for squaraine and having a squaraine with improved spectral response in the visible region are accomplished.

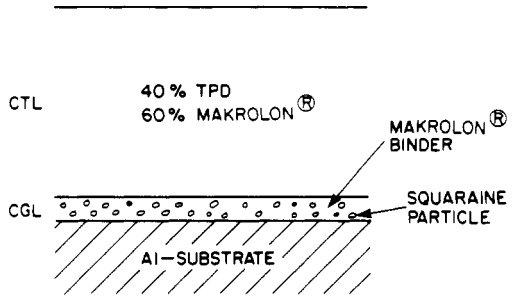

Figure 1. Cross section of a bilayer photoreceptor device of UFSq.

Experimental Section

Materials. 1-(3′,4′-Dimethoxyphenyl)-2-hydroxycyclobutene-3,4-dione was synthesized by a (2 + 2) cycloaddition process as described earlier.[10,11] 3-Fluoro-*N,N*-dimethylaniline was prepared by alkylating *m*-fluoroaniline with trimethyl phosphate.[12] Tributyl orthoformate (TOBF) was purchased from Pfaltz & Bauer. Poly(vinyl formal) (PVF, formal content 82%, acetate content 12%, hydroxy content 6%) was obtained from Scientific Polymer Products, Inc. Makrolon was a polycarbonate from Mobay Chemical Co. The hole-transporting compound *N,N′*-diphenyl-*N,N′*-bis(3-methylphenyl)-1,1′-biphenyl-4,4′-diamine, TPD, was obtained from an internal source, and the synthesis of TPD has been reported elsewhere.[13] Methylene chloride, chloroform, 2-propanol and tetrahydrofuran were certified grade and ether was anhydrous grade. All these solvents were obtained from Fisher and were routinely stored over 3-Å molecular sieves prior to use.

General Techniques. Visible absorption spectra (400–820 nm) were recorded on a Hewlett-Packard 8451 diode array spectrophotometer. X-ray powder diffraction patterns were obtained in-house on a Scintag PAD V X-ray diffractometer. Particle size and particle morphology of squaraine pigments were studied by scanning electron microscopy (SEM) on a Philips 501B instrument.

Syntheses of UFSq. (a) Direct Method. 1-(3′,4′-Dimethoxyphenyl)-2-hydroxycyclobutene-3,4-dione (2.34 g, 0.01 mol), 3-fluoro-*N,N*-dimethylaniline (1.45 g, ~0.01 mol), tributyl orthoformate (7.5 mL), and 80 mL of 2-propanol were charged into a 300-mL three-neck flask, which was stirred and brought to reflux under a nitrogen atmosphere at an oil bath temperature of 100–105 °C. After 100 min, the mixture was cooled to room temperature. The precipitated dark blue product was isolated by filtration. The product was purified by washing with cold 2-propanol until the filtrate was light blue. After an ether rinse, the product was vacuum dried, yielding 2.05–2.15 g (57–60%) of a blue solid, which was subsequently identified as UFSq.[10]

(b) Salt Method. Equivalent amounts of 1-(3′,4′-dimethoxyphenyl)-2-hydroxycyclobutene-3,4-dione and 3-fluoro-*N,N*-dimethylaniline were mixed in tetrahydrofuran to form a salt as previously described.[10] The salt (6.6 g, 7.7 mmol) was suspended in a 300-mL three-neck flask containing 14.3 mL of tributyl orthoformate and 150 mL of 2-propanol. The stirred mixture was kept at reflux under a nitrogen atmosphere for ~100 min. A dark blue precipitate was formed. The mixture was cooled to room temperature. The solid product was isolated and purified as

(4) Law, K. Y.; Facci, J. F.; Bailey, F. C.; Yanus, J. F. *J. Imaging Sci.* **1990**, *34*, 31.
(5) Wingard, R. E. *IEEE Ind. Appl.* **1982**, 1251.
(6) Sprenger, H. E.; Zeigenbein, W. *Angew. Chem., Int. Ed. Engl.* **1966**, *5*, 894.
(7) Law, K. Y. U.S. Patent 4,524,219, 1985.
(8) Law, K. Y.; Bailey, F. C. *Can. J. Chem.* **1986**, *64*, 2269.
(9) Paine, A. J. *Tetrahedron Lett.* **1984**, *25*, 135 and references therein.
(10) Law, K. Y.; Bailey, F. C. *J. Chem. Soc., Chem. Commun.* **1990**, 863.
(11) Law, K. Y.; Bailey, F. C. *J. Org. Chem.*, submitted.
(12) Vogel, A. I. (Revised by Furniss, B. S.; Hannaford, A. J.; Roger, V.; Smith, P. W. G.; Tatchell, A. R.) *Textbook of Practical Organic Chemistry*, 4th ed.; Longman: London, 1978; Chapter IV.
(13) Stolka, M.; Yanus, J. F.; Pai, D. M. *J. Phys. Chem.* **1984**, *88*, 4707.

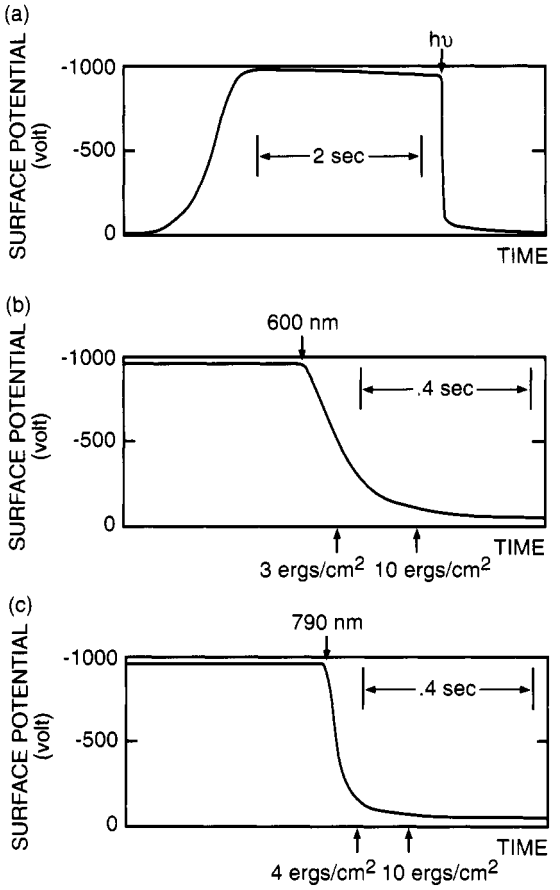

Figure 2. Photodischarge curves of a bilayer device of UFSq: (a) dark decay measurement, (b) and (c) photosensitivity measurements at 600 and 790 nm, respectively.

described above, yield UFSq 3.6–3.8 g (57–60%).

Device Fabrication and Xerographic Measurements. The xerographic properties of UFSq were studied in bilayer xerographic devices. A schematic of the cross section of a bilayer device is shown in Figure 1. Typical formulations for the UFSq dispersion and the TPD coating solution are summarized as follows: (1) UFSq dispersion: 52.8 mg of PVF; 211.2 mg of UFSq; 10 mL of methylene chloride; ~85 g of steel shot (1/8-in. diameter). (2) TPD coating solution: 4.2 g of Makrolon; 31 mL of methylene chloride; 2.8 g of TPD.

The UFSq dispersion was prepared by first dissolving 52.8 mg of PVF in 10 mL of methylene chloride in a 1-oz brown bottle. UFSq (211.2 mg) and steel shot (~85 g, 1/8-in. diameter, 302 grade from Superior Ball Co., washed with methanol and methylene chloride before use) were added to the polymer solution. The brown bottle was then placed in a Red Devil Paint Conditioner (Model 5100X) and was shaken for 2 h. The resulting dispersion was coated onto a 7.5 in. × 10 in. precleaned brush-grained aluminum substrate (from Ron Ink, Co.) using a Gardner Mechanical Drive with a 6-in.-wide 0.5-mil Bird Film Applicator inside a humidity-controlled glovebox. The relative humidity of the glovebox was controlled by dry air and was less than 25% for all the coatings used in this work. The resulting charge generation layer (CGL) was air-dried for ~30 min and vacuum-dried (2 mmHg) at ~100 °C for ~1 h before further coating. The thickness of the CGL was ~0.4 μm as estimated from cross-section TEM micrographs.

The charge-transporting layer (CTL) was obtained by coating the TPD solution onto the CGL using a 3.5-in.-wide 5-mil wet gap Bird Film applicator. The resulting bilayer device was air-dried for ~0.5 h and vacuum-dried (2 mmHg) at ~100 °C for ~16 h before electrical testings. The thickness of the CTL was ~26 μm as estimated from TEM micrographs.

Xerographic measurements were made on a flat plate scanner using 2 in. × 2.5 in. samples. Typically, the bilayer device was charged negatively to about −1000 V by a corotron device. The surface potential of the device was monitored with a capacitively coupled ring probe connected to a Keithley electrometer (Model 610C) in the Coulomb mode. The output of the electrometer was displayed on a strip chart recorder (HP Model 740A) which was calibrated by applying a known voltage on an uncoated aluminum substrate. The exposure wavelength and the intensity were selected and adjusted using interference and neutral density filters, respectively. With the shutter closed, the dark decay of the device ($\Delta V/\Delta t$) was measured. With the shutter open, the device could be exposed to an intense erase light to determine the residual potential (V_R) or to a monochromatic light of known intensity (I in ergs/(cm^2 s)) to determine the photosensitivity of the device. Typical outputs of a dark decay measurement and photosensitivity measurements for a UFSq bilayer device are given in Figures 2. The photosensitivity of the device is expressed as $E_{0.5}$, the energy required to photodischarge half of the initial surface potential (V_i). $E_{0.5}$ is the product of I and t, where t is the time for I to photodischarge the device from V_i to $^1/_2V_i$.

Scheme I

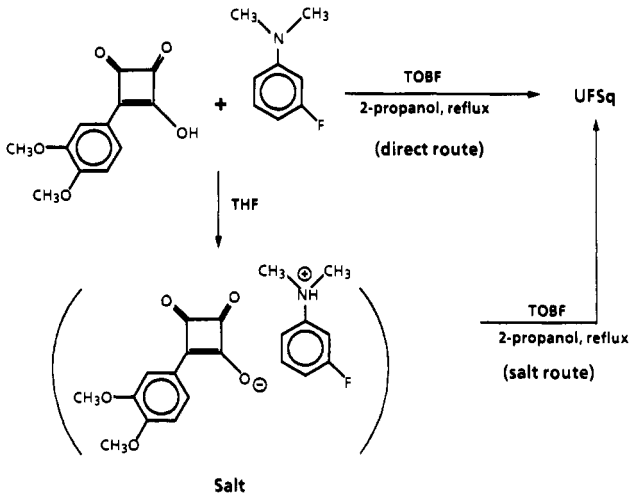

Results and Discussion

Synthesis, Purification, and Solid-State Properties. *Synthesis and Purification.* Condensation of 1-(3′,4′-dimethoxyphenyl)-2-hydroxycyclobutene-3,4-dione, which was prepared by a (2 + 2) cycloaddition reaction between, 3,4-dimethoxyphenyl ketene and tetraethoxyethylene followed by an acid hydrolysis, with 3-fluoro-*N*,*N*-dimethylaniline in refluxing 2-propanol in the presence of a drying reagent [6 equiv of tributyl orthoformate (TOBF)] yields UFSq as a dark blue precipitated solid. The condensation reaction can be accomplished by directly condensing the two reactants in refluxing 2-propanol or indirectly by first forming the salt of the two reactants and then condensing the salt thereafter. The isolated yields of UFSq in both routes are identical, 57–60%. Details on the optimization of reaction conditions and mechanism of the synthesis will be reported elsewhere.[11] The reaction scheme for the synthesis is depicted in Scheme I. Satisfactory analyses, similar melting points, and identical spectroscopic data (IR, vis absorption, NMR) were obtained from UFSq samples of both routes.

UFSq exhibits reasonably good solubility in chlorinated solvents, especially at their boiling temperatures. In this work, we purify UFSq by solvent extraction using a Soxhlet apparatus. Methylene chloride and chloroform were chosen as extraction solvents. Under our experimental conditions, UFSq precipitates as a reflective silver-blue solid and was recovered by filtration. The recovery was ~80–90%. While the elemental analyses and the spectroscopic properties of the as-synthesized and the purified samples are virtually indistinguishable, their melting points are varied, with the as-synthesized samples being the

Figure 3. SEM micrographs of various UFSq samples: (a) as-synthesized, (b) from $CHCl_3$ extraction, (c) from CH_2Cl_2 extraction.

lowest (208–211 °C) and the CH_2Cl_2 extracted sample the highest (220–221 °C). The physical data are summarized in Table I. Since the melting point variation for the three samples in Table I parallels the xerographic performance, with the CH_2Cl_2 sample having the highest melting point and the highest xerographic sensitivity, we conclude that solvent extraction of UFSq purifies the material and that CH_2Cl_2 is the most effective solvent to purify UFSq.

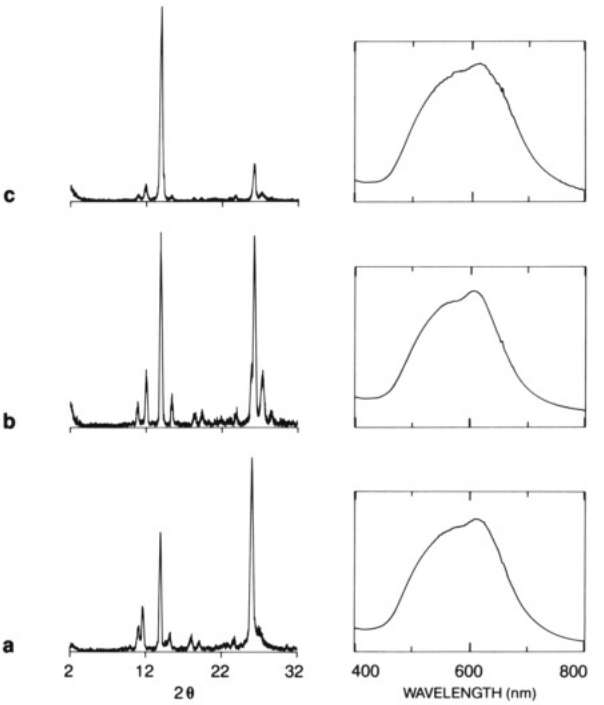

Figure 4. X-ray powder diffraction patterns and solid-state absorption spectra (in KBr pellets) of various UFSq samples: (a) as-synthesized, (b) from $CHCl_3$ extraction, (c) from CH_2Cl_2 extraction.

Solid-State Properties. The size and the shape of the particles of the as-synthesized and the purified samples of UFSq were studied by scanning electron microscopy (SEM). The particle size and the distribution of the as-synthesized samples (by the direct or the salt route) are identical. A representative SEM micrograph is given in Figure 3a. The SEM micrographs of the CH_2Cl_2 purified and the $CHCl_3$ purified samples are given in parts b and c of Figure 3, respectively. A glance at these micrographs reveals that CH_2Cl_2 extraction produces the largest particle size. The particle size of the $CHCl_3$ extraction is larger than the as-synthesized sample, although the size distribution between them is very similar. These physical data are summarized in Table I also. Since the CH_2Cl_2 purified sample not only exhibits the highest melting point, but also the largest particle size, we believe that UFSq is recrystallized during the solvent extraction process, and CH_2Cl_2 extraction of UFSq generates the purest UFSq sample in this work.

The photoconductivity of squaraine in devices has been shown to be governed by its aggregation,[14] and the aggregation can be studied by X-ray diffraction technique and absorption spectroscopy.[4] The data on the X-ray powder diffraction patterns and the solid-state absorption spectra of various UFSq samples (dispersed in clear KBr pellets) are depicted in Figure 4. The X-ray data are tabulated in Table I. In the X-ray powder pattern of the as-synthesized sample, diffraction lines corresponding to d spacings of 3.4, 6.3, and 7.6 Å are observed. In the solid-state absorption spectrum, two bands are observed, one at longer wavelength (~610 nm), the other at shorter wavelength (~565 nm) as compared to the solution absorption maximum (λ_{max} 590 nm in $CHCl_3$[10]). This set of solid-state properties is typical of those of photoconductive squaraines, such as HSq and its derivatives.[2,4] It suggests that UFSq molecules form photoconductive aggregates in

(14) Law, K. Y. *J. Phys. Chem.* **1988**, *92*, 4226.

Table I. Effects of Synthesis and Purification on the Physical and Morphological Properties of UFSq

history	appearance	mp, °C	analysis[b] C	analysis[b] H	analysis[b] N	distribution of particle size, μm	X-ray data d spacing, Å	X-ray data rel intensity
as-synthesized[a]	dark blue	208–211	67.47	5.26	3.85	1.2–16	3.4	100
							6.3	63
							7.6	22
CH_2Cl_2 extraction	light blue	220–221	67.76	5.22	3.86	2.5–36	3.4	90
							6.3	100
							7.4	26
$CHCl_3$ extraction	light blue	214–216	67.38	5.10	3.94	1.5–13	3.4	19
							6.3	100
							7.4	7

[a] There is no difference in physical properties between the direct route and the salt route sample. [b] The calculated values of UFSq are C 67.60, H 5.10, N 3.94.

Table II. Effects of Synthesis and Purification on the Xerographic Properties of UFSq[a]

	as-synthesized direct route	as-synthesized salt route	CH_2Cl_2 purified	$CHCl_3$ purified
charging voltage, kV	−4.80	−4.80	−4.80	−4.90
surface potential, V	−960	−920	−980	−990
dark decay, V/s	−30	−20	−15	−14
V_R, V	−40	−30	−25	−20
$E_{0.5}$, ergs/cm^2				
at 600 nm	6.1	6.8	3.1	4.1
at 790 nm	4.3	4.6	1.9	3.1

[a] CGL: ~0.4 μm thick, 80 wt % of UFSq, 20% PVF. CTL: ~26 μm thick, 40% TPD, 60% Makrolon.

the solid state during the synthesis. As shall be seen in the xerographic data of UFSq, this has been translated into high photosensitivity in xerographic devices.

For the purified samples, their solid-state absorption spectra are identical to the as-synthesized sample. In the X-ray diffraction patterns, the same set of diffraction lines are observed (Figure 4), although there is a variation in relative intensity among them. The fact that the three absorption spectra in Figure 4 are identical indicates that the intermolecular interaction between UFSq molecules in the solid is identical among the three samples. The variation in relative intensity among diffraction lines probably suggest that microcrystals of UFSq may have been preferably grown into different orientations during the recrystallization process. A similar phenomenon was observed earlier, where we showed that HSq was grown in a different orientation by variation of the synthetic condition.[2]

Xerographic Properties. *Time-Zero Electricals.* The xerographic properties of various USFq samples were studied in bilayer photoreceptor devices (Figure 1). Typical photodischarge curves for a device containing CH_2Cl_2-purified UFSq are shown in Figures 2. The xerographic data obtained from these photodischarge curves along with similar data from the as-synthesized sample and the $CHCl_3$ purified sample are summarized in Table II. Our data show that the xerographic properties of the as-synthesized samples are not sensitive to their synthetic history. After purification by solvent extractions, improvements in xerographic performance are obtained. This is indicated by the decreases in dark decay and $E_{0.5}$ values for the extracted samples relative to the as-synthesized samples (Table II). We concluded earlier that solvent extraction improves the purity of the UFSq samples. We thus attribute the improvements in xerographic properties to a purity effect. The highest photosensitivity is obtained from the CH_2Cl_2 purified sample, and this same sample also exhibits the highest melting point. The contribution of sample purity to the sensitivity is evident.

In xerography, photoconductors of low dark decay and high sensitivity are of practical significance because they enable the formation of high-contrast electrostatic images at a high speed.[15] In this regard, squaraines have been known to have a high dark-decay problem for some time.[16,17] As noted in the Introduction, a number of synthetic and purification procedures have recently been developed to circumvent this performance shortfall. Typically, HSq and its derivatives exhibit dark-decay values of −30 to −100 V/s and $E_{0.5}$ values of 3 to >20 ergs/cm^2.[2,14,18] In this work, UFSq is shown to have a dark-decay value of −15 V/s and $E_{0.5}$ values of 3.1 and 1.9 ergs/cm^2 at 600 and 790 nm, respectively, after purification. The significance here is the achievement of dark decay reduction and sensitivity improvement at the same time. The xerographic performance of UFSq surpasses all known squaraines to date. From the photodicharge curve in Figure 2c, one can estimate that the light exposure required to achieve a contrast potential of 600–700 V is ~4 ergs/cm^2 at 790 nm. This sensitivity performance makes UFSq one of the most sensitive IR photoconductor known to date, including the recently reported Y-type titanyl phthalocyanine.[19]

There are many factors that can influence the sensitivity results in bilayer devices. These factors include impurity, particle size, morphology (crystallinity and aggregated form), fabrication effect, and the efficiency of hole injection from the CGL to the CTL.[4] While the effect of impurity on the sensitivity has already been discussed, we have also tried to examine other possible enablers that may be responsible for the high sensitivity observed in this work. We have examined the solubility characteristic and solid-state properties of UFSq and found that they are very similar to those of HSq. We have also examined the particle size and particle distribution of UFSq in devices by TEM microscopy and find no discernible difference between devices of UFSq and HSq. These findings suggest that, particle size, morphology and fabrication effect are not major factors that promote the high sensitivity.

The effect of the efficiency of hole-injection from the CGL to the CTL has been shown to be crucial to the xerographic sensitivity and the efficiency was shown to be assessable by solution electrochemistry.[4,20] UFSq is,

(15) Weigl, J. W. *Angew. Chem., Int. Ed. Engl.* **1977**, *16*, 374.
(16) Chang, M. S. H.; Edelman, P. G. U.S. Patent 4,353,971, 1982.
(17) Chang, M. S. H.; Berman, M. F. U.S. Patent 4,391,888, 1983.
(18) Law, K. Y.; Bailey, F. C. *Dyes. Pigm.* **1988**, *9*, 85.
(19) Fujimaki, Y.; Tadokoro, H.; Oda, Y.; Yoshioka, H.; Homma, T.; Moriguchi, H.; Watanake, K.; Kinoshita, A.; Hirose, N.; Itami, A.; Ikeushi, S. *SPSE Proceedings, The Fifth International Congress on Advances in Non-Impact Printing Technologies*; 1990; p 37.
(20) Melz, R. J.; Champ, R. B.; Chang, L. S.; Chiou, C.; Keller, G. S.; Liclican, L. C.; Neiman, R. B.; Shattuck, M. D.; Weiche, W. J. *Photogr. Sci. Eng.* **1977**, *21*, 73.

Table III. Spectral Sensitivity Data of a Bilayer UFSq Device[a]

	wavelength, nm										
	450	520	550	600	650	700	750	790	800	850	900
$E_{0.5}$, ergs/cm^2	3.5	3.7	4.3	3.1	3.4	2.6	2.4	1.9	3.0	11	66
S, V ergs/cm^2	147	152	118	185	173	221	267	290	184	44	7.3

[a] This is the same CH_2Cl_2 device as in Table II.

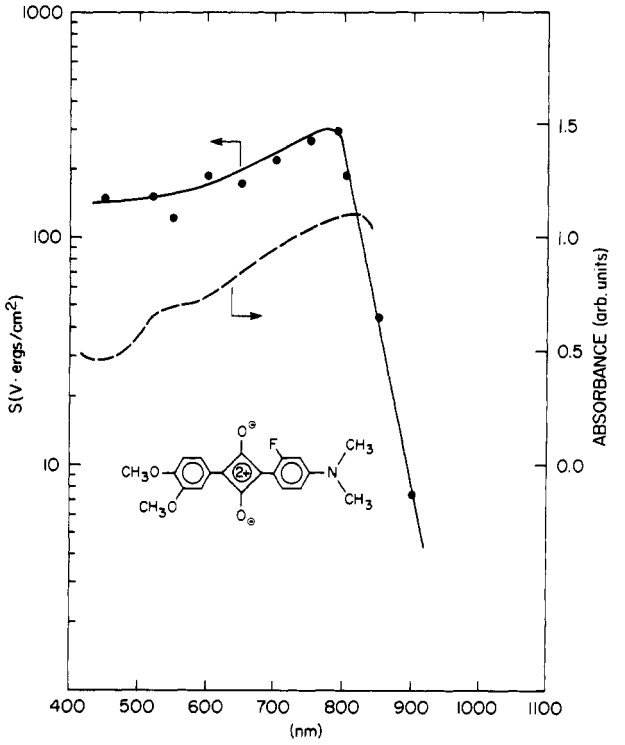

Figure 5. Plots of the spectral sensitivity and the absorption spectrum of UFSq in a bilayer device.

however, not stable electrochemically in solution and its oxidation potential could not be determined.[21] Nevertheless, based on the substituent effect, which is additive, and the fact that UFSq bears a weaker electron-releasing group as compared to HSq, one can safely assume that the oxidation potential of UFSq should be higher than those of HSq and its derivatives.[4] Accordingly, the injection of photogenerated holes in the CGL of UFSq to the TPD CTL should be very efficient. It is therefore probable that the high efficiency of hole injection may partially be responsible for the sensitivity result.

Spectral Response. The spectral sensitivity of UFSq in a bilayer device was obtained by analyzing photodischarge curves at various wavelengths. The $E_{0.5}$ values and the sensitivity (obtained by dividing the slope of the initial photodischarge by the light intensity) at various wavelengths are tabulated in Table III. A plot of the spectral sensitivity along with the absorption spectrum of a UFSq CGL are given in Figure 5. The data indicate that the spectral sensitivity curve of UFSq matches its absorption spectrum.[22] UFSq has a high and flat photoresponse in the visible region (400–650 nm) and a peak sensitivity at 790 nm in xerographic devices. By comparison of a similar plot of HSq (Figure 6), we conclude that an improvement

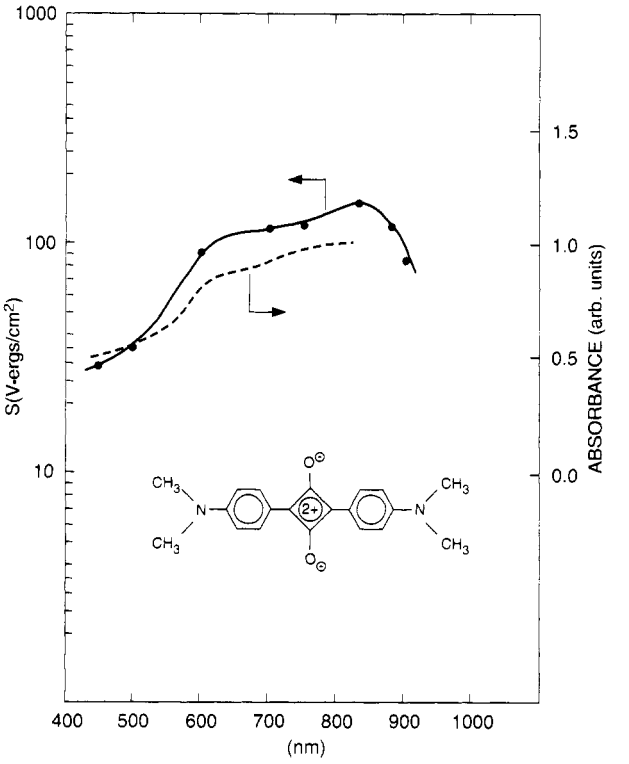

Figure 6. Plots of the spectral sensitivity and the absorption spectrum of HSq in a bilayer device.

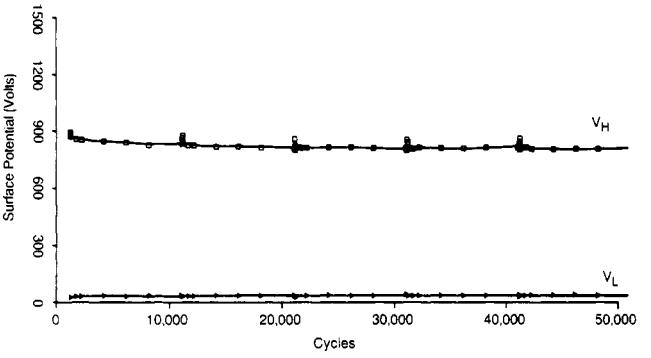

Figure 7. Electrical cycling plot of a UFSq bilayer device.

in spectral response in the visible region, specifically at 400–500 nm, has been obtained.

The monomeric absorption maxima of UFSq and HSq in chloroform are at 590[10] and 624 nm,[23] respectively. The hypsochromic shift observed in UFSq is attributable to the decrease in charge-transfer character in the electronic state of UFSq due to the anisole ring.[10] It is evident from the absorption spectra in Figures 5 and 6 that the hypsochromic shift observed in solution has led to a similar hypsochromic shift in the solid state absorption spectra. This results in an increase in absorbance and an improvement in spectral response at 400–500 nm in the xerographic device.

Finally, one can estimate from the photodischarge curve in Figure 2b that the energy required to achieve a contrast potential of 600 V is 6 ergs/cm^2 at 600 nm. These sensitivity data compare favorably to other leading photogeneration pigments in the visible region, such as azo pigments,[24] perylenes,[25] etc. These results thus suggest

(21) Facci, J. F.; Law, K. Y., unpublished observation.
(22) The CGL is about 0.4 μm thick and consists of small particles of UFSq uniformly distributed within the layer. The absorption spectrum of the CGL is significantly broader than the solid state absorption spectrum given in Figure 4. We believe that the broad spectrum observed in the CGL is a geometrical effect because an identical spectrum can be obtained when the material recovered from the CGL is dispersed in KBr.

(23) Law, K. Y. *Chem. Phys. Lett.* **1988**, *150*, 357.
(24) Ohta, K. *Electrophotography* **1986**, *25*, 83.
(25) Loutfy, R. O.; Hor, A. M.; Kazmaier, P.; Tam, M. *J. Imaging Sci.* **1989**, *33*, 151.

that UFSq should be useful as a photogeneration pigment in copier as well.

Electrical Cycling. To test the durability of UFSq in practical photoreceptor application, a bilayer device of UFSq (CH_2Cl_2 purified)[26] was subjected to a xerographic cycling test on an in-house drum scanner. The speed experienced by the device was ~30 in./s. Basically, the device was subjected to thousands and thousands of charging–photodischarge cycles at a very high rate. In each cycle, the surface potential of the device at 0.2 s after charging, V_H, and the surface potential after light erasure (by a 300 ergs/cm^2 white light source), V_L, were recorded. The results of a 50 000 cycling plot are given in Figure 7. Our data clearly indicate that UFSq is extremely stable electrically. The suitability of using UFSq in practical devices is demonstrated.

Concluding Remarks

This report summarizes results of our investigation on the synthesis, purification, and xerographic properties of UFSq. UFSq can be synthesized by either direct or indirect condensation of 1-(3′,4′-dimethoxyphenyl)-2-hydroxycyclobutene-3,4-dione with 3-fluoro-*N*,*N*-dimethylaniline. Xerographic evaluation showed that the as-synthesized UFSq exhibits a dark decay of −30 V/s and $E_{0.5}$ values of 4.3–6.8 ergs/cm^2 in bilayer photoreceptor devices. Purification of UFSq by solvent extraction, particularly with methylene chloride, improves the purity and consequently the xerographic properties of UFSq. A dark-decay value of −15 V/s and $E_{0.5}$ values of 3.1 and 1.9 ergs/cm^2 at 600 and 790 nm, respectively, have been obtained. Evidence has been obtained that the improvements in xerographic properties may be a combination of the high purity and the high hole-injection efficiency of UFSq, from the CGL to the CTL, in the xerographic device.

A device of UFSq is shown to have panchromatic response from the visible to the near-IR regions as well as excellent 50K cyclic stability. This performance makes UFSq one of the most sensitive panchromatic (visible-IR regions) organic photoconductors known to date, rendering the potential use of UFSq in printers, copiers, and multifunction printer-copiers.

Acknowledgment. I thank F. C. Bailey for his assistance in synthesizing some of the precursors used in this work. Thanks are also due to M. Evan and M. Curtis for X-ray powder diffraction patterns, W. Niedzialkowski for the SEM micrographs, and S. Towers for the cycling experiments.

Registry No. TPD, 65181-78-4; UFSq, 140175-46-8; FC_6H_4-*m*-NMe_2, 2107-43-9; CH_2Cl_2, 75-09-2; 1-(3',4'-dimethoxyphenyl)-2-hydroxycyclobutene-3,4-dione, 126605-20-7.

(26) In the cycling test, a titanized mylar substrate was used in place of the ball-grain aluminum substrate.

Heterophasic Isotope Exchange in Nanoscale Metal Oxide Particles. Lattice Oxygen and Surface OH Groups with Water Vapor (D_2O and $H_2{}^{18}O$)

Yong-Xi Li and Kenneth J. Klabunde*

Department of Chemistry, Kansas State University, Manhattan, Kansas 66506

Received October 29, 1991. Revised Manuscript Received February 21, 1992

Ionic solids MgO, CaO, and Fe_2O_3 exchange surface and lattice oxide anions with $H_2{}^{18}O$ as monitored by pulsed reactor–GC-MS studies. Depending on the temperature, the process can be controlled to exchange only OH, or additional surface lattice O^{2-}, or additionally, interior lattice O^{2-} (up to 16 layers deep). Exchange of surface oxide has an activation energy 5 times lower than exchange of bulk-lattice oxide, and the latter is probably controlled by E_a(diffusion). High surface area, small particle size MgO samples exchange most readily. Exchange studies with D_2O have shown that surface OH can be quantitated by the same pulsed reaction–GC-MS technique. These experiments have allowed the synthesis of isotopically labeled $Mg^{18}O$, which has proven useful for clarifying surface adsorption/decomposition chemistry. An example is given where the $Mg^{18}O$ yielded labeled formic acid in the surface decomposition of an organophosphorus compound, proving that surface and lattice oxide can take part in such adsorption/decomposition processes.

Introduction

In a series of reports on the adsorption/decomposition of organophosphorus compounds on nanoscale MgO particles, it was determined that surface hydroxyl groups as well as lattice oxygen play a role.[1-3] Furthermore, the importance of surface OH in many catalytic processes on basic metal oxide surfaces should not be minimized.[4-6]

Due to the importance of surface OH and possibly lattice oxygen (oxide anions on the surface and in the interior of the bulk) on these adsorption/decomposition/catalytic processes, we decided to investigate isotope exchange of deuterium and water-^{18}O with MgO, CaO, and Fe_2O_3 nanoscale particles, and we report the results herein.

Before presenting these results, some related work should be summarized. Indeed, the mobility of lattice oxygen in oxidation catalysts has been studied in depth, and these studies have shown that for some multivalent

(1) Li, Yong-Xi; Klabunde, K. J. *Langmuir* **1991**, *7*, 1388.
(2) Li, Yong-Xi; Klabunde, K. J. *Langmuir* **1991**, *7*, 1394.
(3) Li, Yong-Xi; Kopper, O.; Maher, A.; Klabunde, K. J. *Chem. Mater.*, in press.
(4) Larson, J. G.; Hall, W. K. *J. Phys. Chem.* **1965**, *69*, 3080.
(5) Lemberton, J. L.; Perot, G.; Guisnet, M. *J. Catal.* **1984**, *89*, 69.
(6) Hoq, M. F.; Nieves, I.; Klabunde, K. J. *J. Catal.* **1990**, *123*, 349 references therein.

0897-4756/92/2804-0611$03.00/0